



Construction of engineered bifunctional enzymes to improve the production of kaempferol in an *in vitro* synthetic biosystem

Zhiping ZHANG¹, Lin XU¹, Li DING¹, Yesen NIE¹, Chenhong ZHAO¹, Xinyue ZHANG^{1,2*} 

Abstract

Kaempferol, an important flavonol, has numerous health-beneficial bioactivities and possesses a great potential for application in medicine, food, and cosmetics industries. To improve the production of kaempferol in an *in vitro* synthetic biosystem, we designed and constructed a panel of bifunctional enzymes by fusing the flavanone 3-hydroxylase (AtF3H) and the flavonol synthase (AtFLS1) of *Arabidopsis thaliana* with different orientation and different peptide linker type and length. By comparing the output of kaempferol, we obtained a highly active bifunctional enzyme AtF3H-(GGGGS)₂-AtFLS1 with a *K_m* value of 0.129 ± 0.016 mM. After optimization of a series of reaction parameters, kaempferol was produced at 100.54 ± 0.54 mg/L, the currently highest kaempferol output in an *in vitro* synthetic biosystem, and the substrate conversion rate was $68.26\% \pm 0.05\%$. In addition, we observed substrate inhibition for the AtFLS1, which eventually limited the production of kaempferol. This study provides a highly active biocatalyst for production of kaempferol and an insight into biosynthesis of other valuable molecules.

Keywords: kaempferol; flavanone 3-hydroxylase; flavonol synthase; bifunctional enzyme; peptide linker.

Practical Application: Bifunctional enzymes AtF3H-(GGGGS)₂-AtFLS1 exhibited the highest activity in converting naringenin into kaempferol by one-step. The activity of AtFLS1 was inhibited by its substrate dihydrokaempferol. Kaempferol was produced at the currently highest output of 100.54 ± 0.54 mg/L in an *in vitro* synthetic biosystem.

1 Introduction

Flavonoids, a large class of structurally diverse secondary metabolites derived from plants, possess numerous health-beneficial biological activities. Structurally, flavonoids can be grouped into six major subclasses based on the variation in the oxidation state and substitution pattern of the C-ring: flavones, isoflavones, flavonols, flavanones, flavanols (the catechins), and anthocyanidins (Winkel-Shirley, 2001; Falcone Ferreyra et al., 2012; Kumar & Pandey, 2013). Kaempferol (KMF) is an important flavonol compound and has many pharmaceutical and biological properties, such as anticancer, antioxidant, anti-inflammatory, and antimicrobial activities (Tatsimo et al., 2012; Wang et al., 2018, 2019; Alaca et al., 2022). Therefore, this polyphenolic compound has a great potential for application in medicine, food, and cosmetics industries. Currently, KMF is mainly extracted from traditional plants with organic solvents. However, this approach is labor-intensive and time-consuming due to the low content of KMF in plants, ranging from 0.14 – 55.0 mg/100 g fresh weight (Dabeek & Marra, 2019), which leads to a high production cost and thereby greatly restricts its application in industry (Lin et al., 2014; Agar et al., 2015).

In the current opinion, flavanone 3-hydroxylase (F3H) and flavonol synthase (FLS) are two key enzymes in the biosynthetic pathway of KMF (Malla et al., 2013; Zhang et al., 2018). In this pathway, naringenin (NRN) is used as a substrate and converted to dihydrokaempferol (DHK) by F3H and then to KMF by FLS1. With the emergence and development of synthetic biology, novel approaches and systems are designed and established to

synthesize natural compounds (Andrianantoandro et al., 2006; Forster & Church, 2007; Zhang, 2010; Hodgman & Jewett, 2012). Lyu et al. (2019) set up a yeast cell factory to produce KMF by introducing the pathway genes into *Saccharomyces cerevisiae*. However, the *in vivo* biosystem possesses intrinsic disadvantages in producing natural compounds. It is difficult to accurately control and access the *in vivo* system consisting of complex and self-duplicating living cells. Moreover, it usually needs a long time for fermentation to achieve a high output of the compounds of interest (Subsoontorn et al., 2012; You & Zhang, 2013; Isola et al., 2022). Therefore, scientists are devoted to developing an *in vitro* or a cell-free biosynthetic system, as an alternative strategy, to replace the *in vivo* system for production of natural compounds (Jeong et al., 2019; Tinafar et al., 2019). Recently, we have developed an *in vitro* multienzyme system to synthesize KMF from NRN in one pot at an output of 37.55 ± 1.62 mg/L within only 40-50 min (Zhang et al., 2018, 2019).

In the current study, to further improve the output of KMF produced in our *in vitro* system, we designed and constructed a panel of bifunctional enzymes. These engineered enzymes consisted of the flavanone 3-hydroxylase (AtF3H) fused to the flavonol synthase (AtFLS1) of *Arabidopsis thaliana*. We then screened out a highly active bifunctional enzyme by comparing the catalytic activities of these recombinant biocatalysts and applied the construct in our *in vitro* synthetic biosystem. After optimization of reaction parameters, the output of KMF increased greatly and reached up to 100.54 ± 0.54 mg/L. To our

Received 08 Dec., 2022

Accepted 11 Jan., 2023

¹ College of Bioscience and Biotechnology, Yangzhou University, Yangzhou, Jiangsu, China

² Joint International Research Laboratory of Agriculture & Agri-Product Safety, Yangzhou University, Yangzhou, Jiangsu, China

*Corresponding author: zhangxinyue@yzu.edu.cn; zhanglabsubmission@163.com

best knowledge, this study reports the highest output in an *in vitro* biosystem for production of KMF.

2 Materials and methods

2.1 Construction of recombinant plasmids

The primers used for amplification of DNA fragments by polymerase chain reaction (PCR) were listed in Supplementary Material (Table S1) and ordered from GENEWIZ China & Suzhou Lab. Overlap extension PCR was performed to amplify and fuse *Atf3h* (GenBank accession no. **NM_114983.3**) and *Atfls1* (GenBank accession no. **NM_120951.3**) genes according to the published protocol (Hilgarth & Lanigan, 2019). The gel-purified fragments were then cloned into a prokaryotic expression vector pET-32a(+) using a seamless ligation kit (Vazyme Biotech Co., Nanjing, China). The coding sequences for AtF3H and AtFLS1 were connected by a short nucleotide sequence (5'-GGATCCGAATTC-3') consisting of a *Bam*HI site closely linked to an *Eco*RI site. When constructing other recombinant plasmids expressing a bifunctional protein with a different type and length of peptide linker, the nucleotide sequence encoding the linker was inserted between these two restriction sites as per the published protocol (Moffat et al., 2006).

2.2 Expression and purification of a bifunctional enzyme

The recombinant bifunctional enzymes were expressed and purified according to our previous protocol with slight modifications (Zhang et al., 2018). In brief, a recombinant plasmid was transformed into *Escherichia coli* BL21(DE3), followed by inoculating colonies into LB broth with antibiotics. Three milliliters of overnight culture were transferred into 300 mL of LB broth with antibiotics and cultured at 220 rpm and 37 °C. When the optical density at 600 nm reached 0.4–0.6, 0.2 mM isopropyl- β -D-thiogalactopyranoside (IPTG) was added into the culture to induce gene expression at 20–22 °C for 3–4 h. Then, *E. coli* was harvested by centrifugation and resuspended in bacterial lysis buffer containing protease inhibitors, followed by sonication and centrifugation. The supernatant was subjected to purification of His-tagged fusion proteins using nickel nitrilotriacetic acid (Ni-NTA) sepharose (Beyotime Biotechnology, Shanghai, China). The purification was carried out as per the manual instructions and protein purity was determined by sodium dodecyl sulfate–polyacrylamide gel electrophoresis (SDS-PAGE). Coomassie blue staining was performed to visualize the protein bands.

2.3 Enzyme assays

The enzyme assays were performed following our previous protocols with slight modifications (Zhang et al., 2018, 2019). The reaction buffer contained 100 mM Tris-HCl (pH 7.2), 0.4% sodium ascorbate, 10% glycerol, 8.2 mM α -ketoglutaric acid, and 0.01 mM FeSO₄. All enzyme assays in this study were carried out in a volume of 100 μ L in 2-mL tubes containing NRN and the bifunctional enzyme in the reaction buffer. The 2-mL tubes remained open and were incubated in a 40 °C shaking heat block at 600 rpm. All reactions were terminated by adding 10 μ L of acetic acid, followed by adding 100 μ L of ethyl acetate for extraction of flavonoids. After a 2-h extraction, the organic

phase was transferred into a 1.5-mL tube for air drying in a hood. Then, 100 μ L of methanol was added to redissolve the flavonoids in the tubes and the solution was subjected to analysis of flavonoids by high performance liquid chromatography and electrospray ionization mass spectrometry (HPLC/ESI-MS) analysis (Zhang et al., 2018, 2019).

2.4 HPLC/ESI-MS analysis

The HPLC/ESI-MS analysis was performed following our previous protocols to measure the flavonoids in the reaction mixtures (Zhang et al., 2018, 2019).

2.5 Determination of the Michaelis–Menten constant K_m of a bifunctional enzyme

The K_m value of AtF3H-(GGGGGS)₂-AtFLS1 was determined following our previous protocol with slight modifications (Zhang et al., 2018). In brief, the substrate NRN was diluted in the reaction buffer to prepare a series of concentrations, including 0.05 mM, 0.1 mM, 0.15 mM, 0.20 mM, and 0.25 mM, respectively. The measurement was repeated three times and the reaction products were subjected to HPLC analysis. The HPLC data was used to calculate the K_m value using the software OriginPro v9.0 and the value was expressed as mean \pm standard deviation.

2.6 Optimization of a biosynthetic system for producing KMF *in vitro*

We initially set up the *in vitro* biosynthetic system according to our published protocols with slight modifications (Zhang et al., 2018, 2019). In brief, the system contained 100 mM Tris-HCl (pH 7.2), 0.4% sodium ascorbate, 10% glycerol, 8.2 mM α -ketoglutaric acid, 0.01 mM FeSO₄, 0.5 mM NRN, and 50 μ g/mL bifunctional enzyme in a 2-mL reaction tube. The tube was incubated in a 40 °C shaking heat block at 600 rpm for 40 min.

Then, several reaction parameters were optimized to improve the output of KMF. To explore the optimum reaction temperature, the reaction was carried out for 40 min at 25 °C, 30 °C, 35 °C, 40 °C, and 45 °C, respectively. To investigate the optimum reaction time, the reaction was incubated at an optimum temperature for 0 min, 10 min, 20 min, 30 min, 40 min, 50 min, and 60 min, respectively. To probe the optimum substrate concentration, we made a series of reactions containing 0.05 mM, 0.1 mM, 0.2 mM, 0.3 mM, 0.4 mM, and 0.5 mM NRN, respectively. The reactions were then incubated at an optimum temperature for an optimum time. To optimize enzyme amount, we made a series of reactions containing 50 μ g/mL, 100 μ g/mL, 150 μ g/mL, 200 μ g/mL, and 250 μ g/mL bifunctional enzyme, respectively. The reactions contained an optimum concentration of NRN and were incubated at 35 °C for 40 min. In the end, to further explore the optimum substrate concentration and bifunctional enzyme amount in the system, we fixed the ratio of substrate concentration (mM) to enzyme amount (μ g) at 1:25. Shown in Table 1 were the concentrations of the substrate NRN and the bifunctional enzyme added into the reactions. The reaction tubes were incubated at 35 °C for 40 min. All of the flavonoids in the reaction tubes were subjected to HPLC/ESI-MS analysis.

Table 1. Optimization of the substrate concentration and total enzyme amount.

Group #	1	2	3	4	5	6	7	8
Substrate concentration (mM)	0.2	0.4	0.8	1.0	1.2	1.4	1.6	1.8
Enzyme concentration ($\mu\text{g}/\text{mL}$)	50	100	200	250	300	350	400	450

*No.

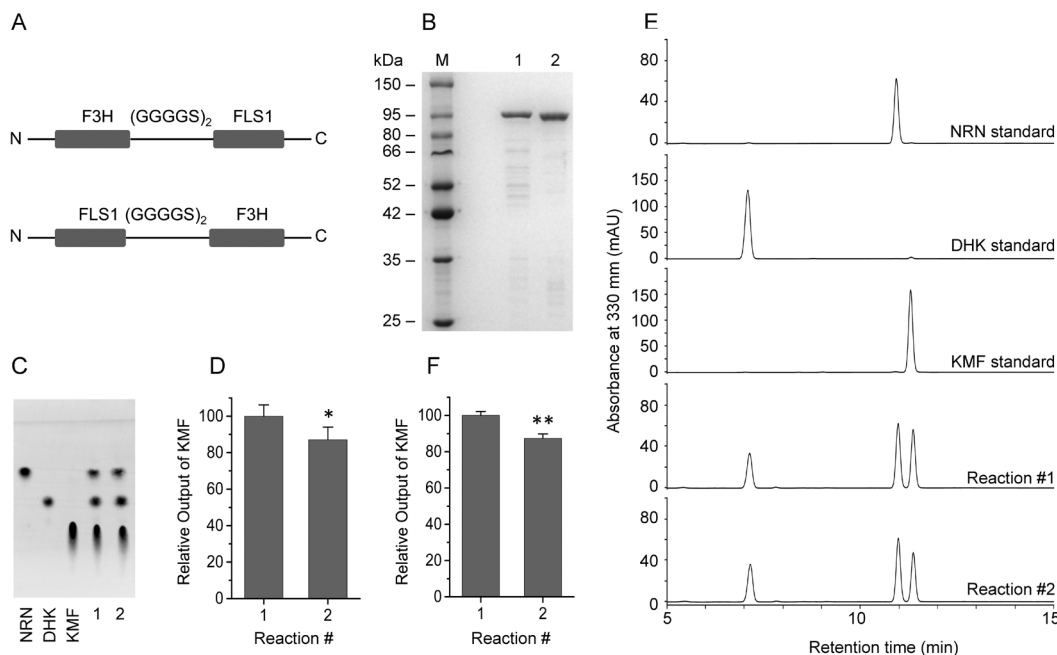


Figure 1. Effect of the orientation of AtF3H and AtFLS1 on the catalytic activity of the bifunctional enzymes. (A) Schematic representation of the structures of recombinant proteins containing AtF3H and AtFLS1 linked by a (GGGGS)₂ peptide. (B) SDS-PAGE analysis of the purified recombinant proteins. M, protein markers; lane 1, AtF3H-(GGGGS)₂-AtFLS1; lane 2, AtFLS1-(GGGGS)₂-AtF3H. (C, D) Polyamide TLC (C) and gray density (D) analyses of the flavonoids in the reaction mixture. (E) HPLC chromatograms of the flavonoids in the reaction mixture. (F) Analysis of the relative KMF yields using the HPLC data. 1, AtF3H-(GGGGS)₂-AtFLS1-catalyzed reaction; 2, AtFLS1-(GGGGS)₂-AtF3H-catalyzed reaction. *No.; * $P < 0.05$; ** $P < 0.01$.

2.7 Statistical analysis

Results were represented as mean \pm standard deviation. The significance of the difference between the values of two groups was evaluated with the 2-tailed Student *t*-test. Statistical significance was assigned to a *P* value lower than 0.05 (*) or 0.01 (**).

3 Results

3.1 The orientation of AtF3H and AtFLS1 in the bifunctional enzyme

To obtain a highly active bifunctional enzyme, we investigated the effect of the orientation of two building blocks AtF3H and AtFLS1 on the enzyme activity of the construct. Two plasmids pET-32a-AtF3H-(GGGGS)₂-AtFLS1 and pET-32a-AtFLS1-(GGGGS)₂-AtF3H were constructed (Figure 1A) and individually transformed into *E. coli* BL21(DE3) for the expression of recombinant proteins AtF3H-(GGGGS)₂-AtFLS1 and AtFLS1-(GGGGS)₂-AtF3H. The proteins were purified by metal chelate affinity chromatography using Ni-NTA sepharose. The purified proteins showed a high purity on an SDS-PAGE gel (Figure 1B).

Then, we compared the enzymatic activity of these two recombinant proteins. HPLC data showed that the relative output

of KMF in the AtF3H-(GGGGS)₂-AtFLS1-catalyzed reaction was higher than that in the AtFLS1-(GGGGS)₂-AtF3H-catalyzed reaction ($P < 0.01$) (Figures 1E, 1F and 2). Similarly, TLC data also demonstrated that the AtF3H-(GGGGS)₂-AtFLS1 produced more KMF than the AtFLS1-(GGGGS)₂-AtF3H in the *in vitro* biosynthetic system ($P < 0.05$) (Figure 1C and 1D). These data indicated that the AtF3H-(GGGGS)₂-AtFLS1 is more active than the AtFLS1-(GGGGS)₂-AtF3H.

3.2 The peptide linker in the bifunctional enzyme

In general, a peptide linker can be roughly classified into two types: flexible and rigid. The type and length of a peptide linker affect the catalytic activity of the construct. To explore the appropriate peptide linker connecting AtF3H and AtFLS1, we designed and constructed a panel of recombinant enzymes containing different peptide linker type and length and then assessed their relative catalytic activity to convert NRN into KMF by comparing the output of KMF. In this study, we chose commonly-used GGGGS as a flexible peptide linker and EAAAK as a rigid one and fused AtF3H and AtFLS1 with various repeats of each linker, respectively. The bifunctional enzymes were expressed in BL21(DE3) and purified by nickel chelate affinity

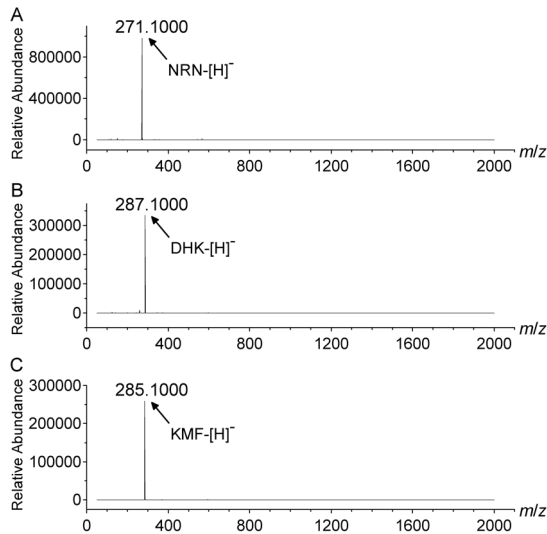


Figure 2. ESI-MS analysis profile of the flavonoid compounds in the reaction mixtures. (A) Exact mass of NRN $[M - H]^-$ $[m/z]^-$ (271.1000). (B) Exact mass of DHK $[M - H]^-$ $[m/z]^-$ (287.1000). (C) Exact mass of KMF $[M - H]^-$ $[m/z]^-$ (285.1000).

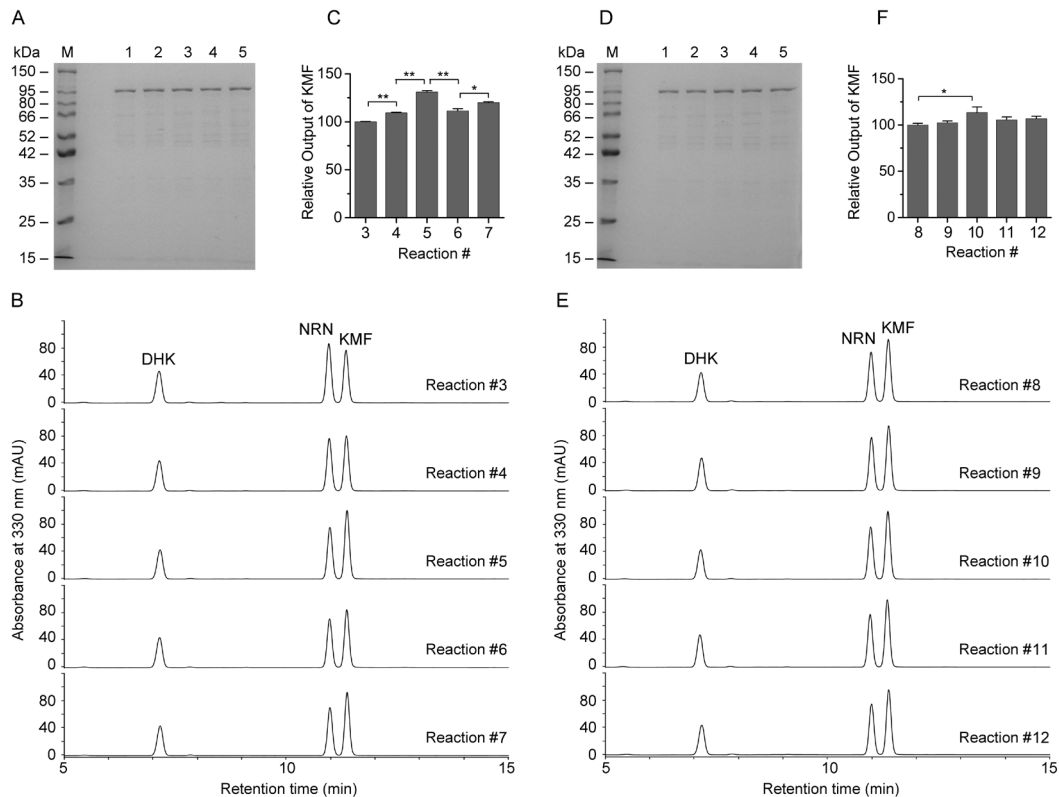


Figure 3. Effect of the type and length of the peptide linker on the catalytic activity of the bifunctional recombinant enzymes. (A) SDS-PAGE analysis of the purified recombinant proteins with a flexible linker (GGGGS)_n (n = 0 – 4). M, protein markers; lane 1, AtF3H-(GGGGS)₀-AtFLS1; lane 2, AtF3H-(GGGGS)₁-AtFLS1; lane 3, AtF3H-(GGGGS)₂-AtFLS1; lane 4, AtF3H-(GGGGS)₃-AtFLS1; lane 5, AtF3H-(GGGGS)₄-AtFLS1. (B, C) HPLC chromatograms of the flavonoids in the AtF3H-(GGGGS)_n-AtFLS1-catalyzed reaction mixture (B) and analysis of the relative KMF yields based on the HPLC data (C). 3, AtF3H-(GGGGS)₀-AtFLS1-catalyzed reaction; 4, AtF3H-(GGGGS)₁-AtFLS1-catalyzed reaction; 5, AtF3H-(GGGGS)₂-AtFLS1-catalyzed reaction; 6, AtF3H-(GGGGS)₃-AtFLS1-catalyzed reaction; 7, AtF3H-(GGGGS)₄-AtFLS1-catalyzed reaction. (D) SDS-PAGE analysis of the purified recombinant proteins with a rigid linker (EAAAK)_n (n = 0 – 4). M, protein markers; lane 1, AtF3H-(EAAAK)₀-AtFLS1; lane 2, AtF3H-(EAAAK)₁-AtFLS1; lane 3, AtF3H-(EAAAK)₂-AtFLS1; lane 4, AtF3H-(EAAAK)₃-AtFLS1; lane 5, AtF3H-(EAAAK)₄-AtFLS1. (E, F) HPLC chromatograms of the flavonoids in the AtF3H-(EAAAK)_n-AtFLS1-catalyzed reaction mixture (E) and analysis of the relative KMF yields using the HPLC data (F). 8, AtF3H-(EAAAK)₀-AtFLS1-catalyzed reaction; 9, AtF3H-(EAAAK)₁-AtFLS1-catalyzed reaction; 10, AtF3H-(EAAAK)₂-AtFLS1-catalyzed reaction; 11, AtF3H-(EAAAK)₃-AtFLS1-catalyzed reaction; 12, AtF3H-(EAAAK)₄-AtFLS1-catalyzed reaction. #No.; **P* < 0.05; ***P* < 0.01.

chromatography. The purified proteins showed a high purity on an SDS-PAGE gel (Figure 3A and 3D). The enzyme activity of each construct was compared against that of AtF3H-AtFLS1 without either GGGGS or EAAAK. Overall, the recombinant proteins with two repeats of a linker had a higher enzyme activity than those with any other repeats in either flexible (*P* < 0.01) or rigid (*P* < 0.05) groups (Figure 3). Among all the constructs, the AtF3H-(GGGGS)₂-AtFLS1 produced more KMF (Figure 3 and Supplementary Material Figure S1) (*P* < 0.01). These data indicated that (GGGGS)₂ is the best linker for the construction of a bifunctional enzyme containing AtF3H and AtFLS1.

3.3 The Michaelis–Menten constant (*K_m*) of the AtF3H-(GGGGS)₂-AtFLS1

To characterize the construct AtF3H-(GGGGS)₂-AtFLS1, we measured its *K_m* value. Our data showed that $11.13 \pm 0.40 \mu\text{g}$ of the AtF3H-(GGGGS)₂-AtFLS1 was required for conversion of $1 \mu\text{mol}$ of NRN into KMF per minute at 40°C and the *K_m* value was calculated to be $0.129 \pm 0.016 \text{ mM}$.

3.4 The optimum reaction temperature

In this study, we set up an *in vitro* synthetic biosystem using the construct AtF3H-(GGGGG)₂-AtFLS1 and then optimized a panel of reaction parameters to improve the output of KMF. Firstly, we explored the effect of reaction temperature on the output of KMF. The temperature varied from 25 °C to 45 °C at intervals of 5 °C. Initially, the output of KMF increased gradually as the reaction temperature went up to 35 °C. However, when the temperature went up further, the output of KMF declined sharply ($P < 0.01$) (Figures 4A and 4B, Supplementary Material Figures S2A and S2B), indicating that a reaction temperature of 35 °C is optimal for this system and higher temperature will inactivate the bifunctional enzyme. As expected, with the increase in the temperature, the amount of NRN left in the reaction mixture gradually decreased and then increased.

3.5 The optimum reaction time

Next, we optimized the reaction time. With the extension of time, the output of KMF went up sharply within the first 30 min ($P < 0.01$) and reached a plateau at 40 min (Figures 4C and 4D, Supplementary Material Figures S2C and S2D), indicating that the optimum reaction time is 40 min for this system and further extension of the reaction time is unnecessary.

3.6 The optimum substrate concentration

Then, we explored the optimum substrate concentration. The concentration of the recombinant enzyme AtF3H-(GGGGG)₂-AtFLS1 was fixed at 50 µg/mL in the reaction. As shown in Figures 4E and 4F and Supplementary Material Figures S2E and S2F, the output of KMF went up gradually when the concentration of NRN increased from 0.05 mM to 0.2 mM; however, higher substrate concentration did not increase but decreased the output of KMF when the concentration of NRN was over 0.3 mM, indicating that the optimum concentration of NRN is 0.2 mM in the biosynthetic system containing 50 µg/mL AtF3H-(GGGGG)₂-AtFLS1. Interestingly, the concentration of DHK went up continuously with a gradual increase in the NRN concentration in the reaction. These data implied that at least one of the building blocks might be inhibited by a high concentration of its substrate. To address the hypothesis, we investigated the effect of substrate concentration on the catalytic activity of the corresponding enzyme. For the 50 µg/mL AtF3H-catalyzed reaction, the output of DHK increased gradually as the concentration of NRN went up to 0.4 mM, but did not further increase as the substrate concentration was over 0.4 mM, indicating that the substrate NRN shows no obvious inhibitory effect on the enzyme activity of the AtF3H (Supplementary Material Figures S3A and S3C). However, for

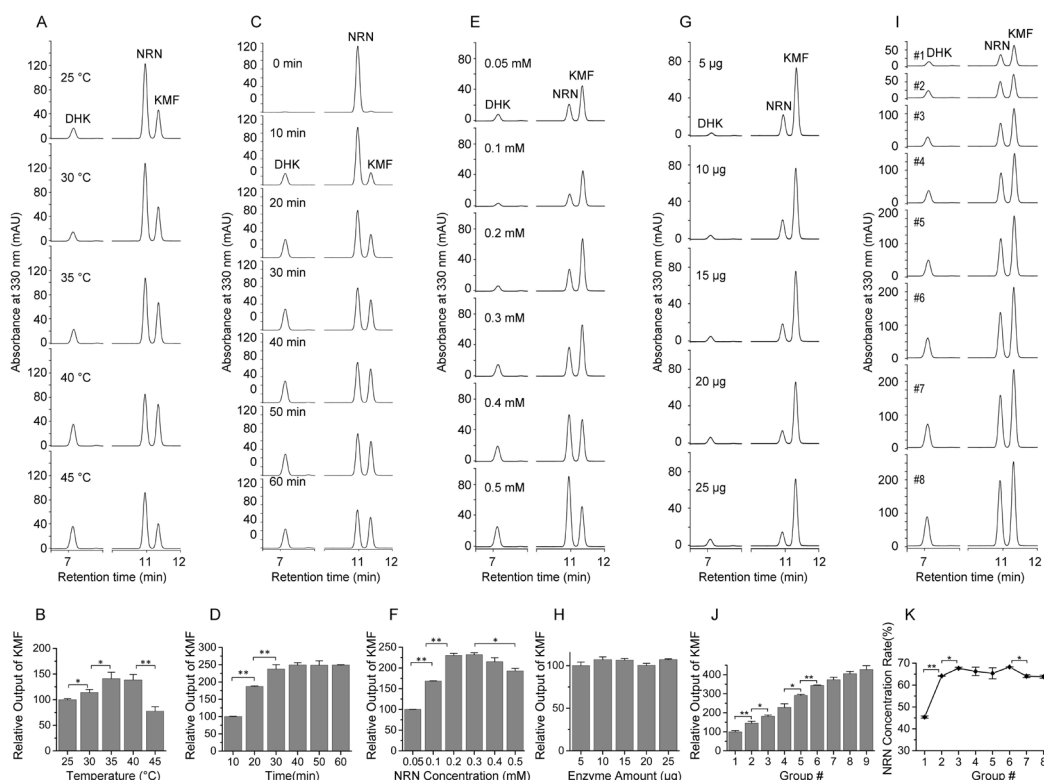


Figure 4. Optimization of the reaction parameters to increase the yield of KMF. (A, B) HPLC analysis of each sample for determining the optimum reaction temperature (A) and analysis of the yield using the HPLC data (B). (C, D) HPLC analysis of each sample for optimizing the reaction time (C) and analysis of the KMF yield using HPLC data (D). (E, F) HPLC analysis of each sample for exploring the optimum substrate concentration in the synthetic system (E) and analysis of the yield using HPLC data (F). (G, H) HPLC analysis for optimizing the total enzyme amount in the synthetic system (G) and analysis of the yield using the HPLC data (H). (I-K) HPLC analysis of each sample (I) for optimizing substrate concentration v.s. total enzyme amount at a same ratio of 1:25 as shown in Table 1 and analysis of the KMF yield (J) and the NRN conversion rate (K) using the HPLC data. Digits 1–8 indicate the reaction numbers in Table 1. *No.; * $P < 0.05$; ** $P < 0.01$.

the AtFLS1-catalyzed reaction, the output of KMF increased initially when the concentration of DHK went up gradually, but decreased when the concentration of DHK was over 0.3 mM (Supplementary Material Figures S3B and S3D), indicating that a high concentration of substrate inhibits the enzyme activity of AtFLS1 and the optimum concentration of DHK is 0.3 mM in the 50 µg/mL AtFLS1-catalyzed reaction.

3.7 The optimum enzyme amount

Subsequently, we investigated the possible effect of enzyme amount on the output of KMF in a 100-µL biosynthetic system containing 0.2 mM NRN and 5 – 25 µg of AtF3H-(GGGGS)₂-AtFLS1. When we increased the enzyme amount in the biosynthetic system, the output of KMF remained almost unchanged (Figures 4G and 4H, Supplementary Material Figures S2G and S2H), but the amounts of NRN and DHK in the reaction mixture gradually decreased and increased, respectively (Figure 4G), indicating that the AtFLS1 catalyzes the rate-limiting step in the conversion of NRN into KMF.

Since a high concentration of DHK inhibits the AtFLS1-catalyzed reaction (Supplementary Material Figures S3B and S3D), we speculated that the output of KMF might further go up if we proportionally increase both substrate concentration and enzyme amount in the reaction system at a fixed ratio. As expected, when the ratio of substrate concentration (mM) to enzyme amount (µg) was fixed at 1:25, the output of KMF increased continuously with the concentration of NRN ranged from 0.2 mM to 1.8 mM (Table 1) (Figures 4I and 4J). Interestingly, with a gradual increase in the concentration of NRN, the substrate conversion rate went up initially ([NRN] < 0.8 mM), subsequently remained almost unchanged ([NRN] = 0.8 – 1.4 mM), and then declined ([NRN] > 1.4 mM) (Figure 4K). These data indicate that the inhibitory effect of the substrate concentration on the output of KMF can be partially overcome by a concomitant increase in the substrate concentration and the enzyme amount at a fixed ratio and the optimum substrate concentration and enzyme amount were 1.4 mM and 0.35 mg/mL, respectively, in our current synthetic biosystem.

3.8 The output of KMF before and after optimization

Finally, we compared the output of KMF before and after optimization. As shown in Figure 5, after optimizing a series of reaction parameters, the substrate conversion rate went up to 68.26% ± 0.05% and the output of KMF increased by 3.43 folds ($P < 0.01$) up to 100.54 ± 0.54 mg/L, which is to date the highest output of KMF in the *in vitro* synthetic biosystem.

4 Discussion

KMF is one of important flavonols found in many plant-derived products and medicinal plants (Calderón-Montaño et al., 2011) and possesses bone-protecting property (Wong et al., 2019). This flavonol is commonly used by food scientists in the development of food additives, dietary supplements, and functional food. Nowadays, many sports person uses dietary KMF supplements or drinks KMF-rich functional beverages to improve their physical strength. Meanwhile, KMF has anti-

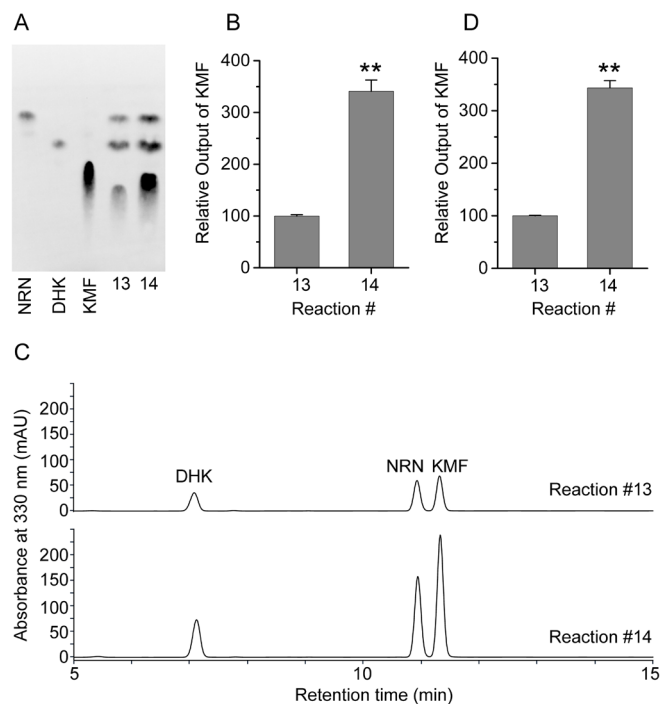


Figure 5. Comparison of the yield of KMF before and after optimization. (A, B) Polyamide TLC (A) and gray density (B) analyses for comparing the KMF yield before and after optimization. (C) HPLC chromatograms of the reaction samples before and after optimization. (D) Analysis of the KMF yield before and after optimization using the HPLC data. 13, before optimization; 14, after optimization. *No.; ** $P < 0.01$.

cancer, anti-oxidant, and anti-inflammatory activities (Calderón-Montaño et al., 2011; Alaca et al., 2022) and a high intake of KMF-rich foods might reduce the risk of developing lung, gastric, pancreatic, and ovarian cancers, as well as cardiovascular diseases and obesity (Calderón-Montaño et al., 2011; Dabeek & Marra, 2019). Therefore, the intake of KMF-rich nutraceuticals is also common in the geriatric population who suffer from various age-related ailments such as cardiovascular diseases, diabetes, and cancers. In spite of the growing market demand for KMF in foods and beverages, this small molecule is usually derived from plants, which limits its application in the food industry due to the high production cost (Periferakis et al., 2022).

Previously, we developed an *in vitro* biosystem for KMF production, but with a relatively low output (Zhang et al., 2018, 2019). In this study, we designed and constructed a panel of recombinant biocatalysts and screened out a highly active bifunctional enzyme AtF3H-(GGGGS)₂-AtFLS1 for KMF production in an *in vitro* biosynthetic system. After optimization of the reaction parameters, the output of KMF reached up to 100.54 ± 0.54 mg/L. To the best of our knowledge, the production of KMF in the study stands for the highest output in an *in vitro* synthetic biosystem.

Among all the bifunctional constructs with different orientation of the building blocks and different type and length of the peptide linker, the recombinant enzyme AtF3H-(GGGGS)₂-AtFLS1 produced more KMF in our current system. This construct contained two repeats of the flexible linker GGGGS with the

AtF3H at the N-terminus and the AtFLS1 at the C-terminus, which probably improved the enzyme activity by helping the recombinant bifunctional enzyme to fold correctly and form a substrate channel (Arai et al., 2001; Yang et al., 2015), thereby leading to a high output of KMF in the system. Moreover, we found that the concentration of DHK in the AtFLS1-(GGGGS)₂-AtF3H-catalyzed reaction was higher than that in the AtF3H-(GGGGS)₂-AtFLS1-catalyzed one, indicating that the former orientation of the building blocks probably had an adverse effect on the enzymatic activity of the AtFLS1, thus resulting in the accumulation of the DHK in the reaction mixture. Furthermore, we found that the AtFLS1 exhibited a remarkable substrate inhibition. As a result, the AtF3H-(GGGGS)₂-AtFLS1 is more active than the AtFLS1-(GGGGS)₂-AtF3H in producing KMF.

When compared with our previous *in vitro* multienzyme synthetic system (Zhang et al., 2018), our current system is more convenient in preparing the biocatalyst and has obvious advantages on the output of KMF and the conversion rate of the substrate. This system also shows many advantages over the traditional plant extraction and the microbial factory. It is not only time- and labor-saving, but also cost-effective. Moreover, it is easy to control the reaction conditions and purify the desired products due to the clearness and simplicity of the components. Most importantly, this system can be easily scaled up for the mass production of KMF and thereby has a great potential for food industrialization.

However, there are still two main limitations in the current production biosystem, which are also our future research directions. First, the bifunctional enzyme is not designed for recycling use, but the preparation of this recombinant construct accounts for the main cost. To resolve this issue, we can immobilize the recombinant enzyme onto inert carriers for repeated use. Second, the output of KMF is still relatively low, especially for industrial scale production. To resolve this issue, further study should be focused on improvement of the enzymatic activities of the building blocks. For F3H, we may improve the enzymatic activity of the AtF3H by gene mutation or screen for more efficient F3H from other plants. For FLS1, we may circumvent the substrate inhibition of the AtFLS1 by gene mutation or screen for more efficient FLS with enzymatic activity not influenced by substrate inhibition from other plants. In addition to the relative low enzymatic activity, this issue might also be caused by the low solubility of KMF in aqueous reaction condition, which can be partially resolved by biosynthesis of KMF in a flow reactor to lower the local concentration of reaction products in the reaction mixture.

5 Conclusions

In this study, a highly active bifunctional enzyme AtF3H-(GGGGS)₂-AtFLS1 was screened out from a panel of recombinant biocatalysts for production of KMF in an *in vitro* system. When the reaction was carried out at 35 °C for 40 min in a 100- μ L volume containing 1.4 mM NRN and 0.35 mg/mL AtF3H-(GGGGS)₂-AtFLS1, the output of KMF reached up to 100.54 \pm 0.54 mg/L, which, to the best of our knowledge, is the highest output in an *in vitro* synthetic biosystem. This study provides a highly active biocatalyst for production of KMF, which facilitates its application in food, cosmetic and medicinal industries.

Abbreviations

AtF3H flavanone 3-hydroxylase of *Arabidopsis thaliana*

AtFLS1 flavonol synthase of *Arabidopsis thaliana*

DNA deoxyribonucleic acid

ESI-MS electrospray ionization mass spectrometry

HPLC high performance liquid chromatography

IPTG isopropyl- β -D-thiogalactopyranoside

K_m Michaelis–Menten constant

KMF kaempferol

NRN naringenin

PCR polymerase chain reaction

SDS-PAGE sodium dodecyl sulfate–polyacrylamide gel electrophoresis

Conflict of interest

The authors declare that they have no known competing financial interests or personal relationships that could have appeared to influence the work reported in this paper.

Funding

This work was supported by Jiangsu Specially-Appointed Professor Start-up Funds, Six Talent Peaks Project in Jiangsu Province [Grant No. 2014-SWYY-016], Postgraduate Research & Practice Innovation Program of Jiangsu Province [Grant No. KYCX21_3206], and the National Natural Science Foundation of China for Young Scientists [Grant No. 81802765].

Author contributions

Zhiping Zhang: Investigation, Methodology, Data curation, Formal analysis, Visualization, Funding acquisition, Writing-Original Draft. **Lin Xu:** Methodology, Investigation, Visualization, Formal analysis. **Lei Chen:** Investigation, Visualization. **Li Ding:** Funding acquisition. **Kai Liao:** Investigation, Visualization. **Yesen Nie:** Investigation, Visualization. **Yanzhi He:** Investigation, Visualization. **Chenhong Zhao:** Visualization. **Xinyue Zhang:** Conceptualization, Supervision, Funding acquisition, Writing-Reviewing and Editing.

Acknowledgements

The authors would like to provide their gratitude to the Testing Center of Yangzhou University for technical support.

References

- Agar, O. T., Dikmen, M., Ozturk, N., Yilmaz, M. A., Temel, H., & Turkmenoglu, F. P. (2015). Comparative studies on phenolic composition, antioxidant, wound healing and cytotoxic activities of selected *Achillea* L. species growing in Turkey. *Molecules (Basel, Switzerland)*, 20(10), 17976–18000. <http://dx.doi.org/10.3390/molecules201017976>. PMID:26437391.

- Alaca, K., Okumuş, E., Bakkalbaşı, E., & Javidipour, I. (2022). Phytochemicals and antioxidant activities of twelve edible wild plants from Eastern Anatolia, Turkey. *Food Science and Technology (Campinas)*, 42, e18021. <http://dx.doi.org/10.1590/fst.18021>.
- Andrianantoandro, E., Basu, S., Karig, D. K., & Weiss, R. (2006). Synthetic biology: new engineering rules for an emerging discipline. *Molecular Systems Biology*, 2(1), 0028. <http://dx.doi.org/10.1038/msb4100073>. PMID:16738572.
- Arai, R., Ueda, H., Kitayama, A., Kamiya, N., & Nagamune, T. (2001). Design of the linkers which effectively separate domains of a bifunctional fusion protein. *Protein Engineering*, 14(8), 529-532. <http://dx.doi.org/10.1093/protein/14.8.529>. PMID:11579220.
- Calderón-Montaño, J. M., Burgos-Moron, E., Perez-Guerrero, C., & Lopez-Lazaro, M. (2011). A review on the dietary flavonoid kaempferol. *Mini-Reviews in Medicinal Chemistry*, 11(4), 298-344. <http://dx.doi.org/10.2174/138955711795305335>. PMID:21428901.
- Dabeek, W. M., & Marra, M. V. (2019). Dietary quercetin and kaempferol: bioavailability and potential cardiovascular-related bioactivity in humans. *Nutrients*, 11(10), 2288. <http://dx.doi.org/10.3390/nu11102288>. PMID:31557798.
- Falcone Ferreyra, M. L., Rius, S. P., & Casati, P. (2012). Flavonoids: biosynthesis, biological functions, and biotechnological applications. *Frontiers in Plant Science*, 3, 222. <http://dx.doi.org/10.3389/fpls.2012.00222>. PMID:23060891.
- Forster, A. C., & Church, G. M. (2007). Synthetic biology projects in vitro. *Genome Research*, 17(1), 1-6. <http://dx.doi.org/10.1101/gr.5776007>. PMID:17151344.
- Hilgarth, R. S., & Lanigan, T. M. (2019). Optimization of overlap extension PCR for efficient transgene construction. *MethodsX*, 7, 100759. <http://dx.doi.org/10.1016/j.mex.2019.12.001>. PMID:32021819.
- Hodgman, C. E., & Jewett, M. C. (2012). Cell-free synthetic biology: thinking outside the cell. *Metabolic Engineering*, 14(3), 261-269. <http://dx.doi.org/10.1016/j.ymben.2011.09.002>. PMID:21946161.
- Isola, L. A., Mahmood, M. H., Yousif, A. Y., Al-Shawi, S. G., Abdelbasset, W. K., Bokov, D. O., & Thangavelu, L. (2022). A review on fermented aquatic food storage quality based on heat treatment and water retention technology. *Food Science and Technology (Campinas)*, 42, e77321. <http://dx.doi.org/10.1590/fst.77321>.
- Jeong, D., Klocke, M., Agarwal, S., Kim, J., Choi, S., Franco, E., & Kim, J. (2019). Cell-free synthetic biology platform for engineering synthetic biological circuits and systems. *Methods and Protocols*, 2(2), 39. <http://dx.doi.org/10.3390/mps2020039>. PMID:31164618.
- Kumar, S., & Pandey, A. K. (2013). Chemistry and biological activities of flavonoids: an overview. *TheScientificWorldJournal*, 2013, 162750. <http://dx.doi.org/10.1155/2013/162750>. PMID:24470791.
- Lin, S., Zhu, Q., Wen, L., Yang, B., Jiang, G., Gao, H., Chen, F., & Jiang, Y. (2014). Production of quercetin, kaempferol and their glycosidic derivatives from the aqueous-organic extracted residue of litchi pericarp with *Aspergillus awamori*. *Food Chemistry*, 145, 220-227. <http://dx.doi.org/10.1016/j.foodchem.2013.08.048>. PMID:24128471.
- Lyu, X., Zhao, G., Ng, K. R., Mark, R., & Chen, W. N. (2019). Metabolic engineering of *saccharomyces cerevisiae* for de novo production of Kaempferol. *Journal of Agricultural and Food Chemistry*, 67(19), 5596-5606. <http://dx.doi.org/10.1021/acs.jafc.9b01329>. PMID:30957490.
- Malla, S., Pandey, R. P., Kim, B. G., & Sohng, J. K. (2013). Regiospecific modifications of naringenin for astragalin production in *Escherichia coli*. *Biotechnology and Bioengineering*, 110(9), 2525-2535. <http://dx.doi.org/10.1002/bit.24919>. PMID:23568509.
- Moffat, J., Grueneberg, D. A., Yang, X., Kim, S. Y., Kloepper, A. M., Hinkle, G., Piqani, B., Eisenhaure, T. M., Luo, B., Grenier, J. K., Carpenter, A. E., Foo, S. Y., Stewart, S. A., Stockwell, B. R., Hacohen, N., Hahn, W. C., Lander, E. S., Sabatini, D. M., & Root, D. E. (2006). A lentiviral RNAi library for human and mouse genes applied to an arrayed viral high-content screen. *Cell*, 124(6), 1283-1298. <http://dx.doi.org/10.1016/j.cell.2006.01.040>. PMID:16564017.
- Periferakis, A., Periferakis, K., Badarau, I. A., Petran, E. M., Popa, D. C., Caruntu, A., Costache, R. S., Scheau, C., Caruntu, C., & Costache, D. O. (2022). Kaempferol: antimicrobial properties, sources, clinical, and traditional applications. *International Journal of Molecular Sciences*, 23(23), 15054. <http://dx.doi.org/10.3390/ijms232315054>. PMID:36499380.
- Subsoontorn, P., Kim, J., & Winfree, E. (2012). Ensemble Bayesian analysis of bistability in a synthetic transcriptional switch. *ACS Synthetic Biology*, 1(8), 299-316. <http://dx.doi.org/10.1021/sb300018h>. PMID:23651285.
- Tatsimo, S. J., Tamokou, D., Havyarimana, L., Csupor, D., Forgo, P., Hohmann, J., Kuate, J. R., & Tane, P. (2012). Antimicrobial and antioxidant activity of kaempferol rhamnoside derivatives from *Bryophyllum pinnatum*. *BMC Research Notes*, 5(1), 158. <http://dx.doi.org/10.1186/1756-0500-5-158>. PMID:22433844.
- Tinafar, A., Jaenes, K., & Pardee, K. (2019). Synthetic biology goes cell-free. *BMC Biology*, 17(1), 64. <http://dx.doi.org/10.1186/s12915-019-0685-x>. PMID:31395057.
- Wang, J., Fang, X., Ge, L., Cao, F., Zhao, L., Wang, Z., & Xiao, W. (2018). Antitumor, antioxidant and anti-inflammatory activities of kaempferol and its corresponding glycosides and the enzymatic preparation of kaempferol. *PLoS One*, 13(5), e0197563. <http://dx.doi.org/10.1371/journal.pone.0197563>. PMID:29771951.
- Wang, X., Yang, Y., An, Y., & Fang, G. (2019). The mechanism of anticancer action and potential clinical use of kaempferol in the treatment of breast cancer. *Biomedicine and Pharmacotherapy*, 117, 109086. <http://dx.doi.org/10.1016/j.biopha.2019.109086>. PMID:31200254.
- Winkel-Shirley, B. (2001). Flavonoid biosynthesis. A colorful model for genetics, biochemistry, cell biology, and biotechnology. *Plant Physiology*, 126(2), 485-493. <http://dx.doi.org/10.1104/pp.126.2.485>. PMID:11402179.
- Wong, S. K., Chin, K. Y., & Ima-Nirwana, S. (2019). The osteoprotective effects of kaempferol: the evidence from in vivo and in vitro studies. *Drug Design, Development and Therapy*, 13, 3497-3514. <http://dx.doi.org/10.2147/DDDT.S227738>. PMID:31631974.
- Yang, G. G., Xu, X. Y., Ding, Y., Cui, Q. Q., Wang, Z., Zhang, Q. Y., Shi, S. H., Lv, Z. Y., Wang, X. Y., Zhang, J. H., Zhang, R. G., & Xu, C. S. (2015). Linker length affects expression and bioactivity of the onconase fusion protein in *Pichia pastoris*. *Genetics and Molecular Research*, 14(4), 19360-19370. <http://dx.doi.org/10.4238/2015.December.29.46>. PMID:26782589.
- You, C., & Zhang, Y. H. (2013). Self-assembly of synthetic metabolons through synthetic protein scaffolds: one-step purification, co-immobilization, and substrate channeling. *ACS Synthetic Biology*, 2(2), 102-110. <http://dx.doi.org/10.1021/sb300068g>. PMID:23656373.
- Zhang, Y. H. (2010). Production of biocommodities and bioelectricity by cell-free synthetic enzymatic pathway biotransformations: challenges and opportunities. *Biotechnology and Bioengineering*, 105(4), 663-677. <http://dx.doi.org/10.1002/bit.22630>. PMID:19998281.
- Zhang, Z., Fan, S., Chen, Z., He, Y., Huang, M., Ding, L., Zhang, Y., Chen, L., & Zhang, X. (2019). Biosynthesis of a flavonol from a flavanone by establishing a one-pot enzymatic cascade. *Journal of Visualized Experiments*, (150). <http://dx.doi.org/10.3791/59336>. PMID:31475963.
- Zhang, Z., He, Y., Huang, Y., Ding, L., Chen, L., Liu, Y., Nie, Y., & Zhang, X. (2018). Development and optimization of an in vitro multienzyme synthetic system for production of kaempferol from naringenin. *Journal of Agricultural and Food Chemistry*, 66(31), 8272-8279. <http://dx.doi.org/10.1021/acs.jafc.8b01299>. PMID:30019587.

Supplementary Material

Supplementary material accompanies this paper.

Figure S1. The peptide linker type and length affected the catalytic activity of the bifunctional recombinant enzymes. **(A, B)** Polyamide TLC **(A)** and gray density **(B)** analyses of the flavonoid compounds in the AtF3H-(GGGGS)_n-AtFLS1-catalyzed reaction mixture. 3, AtF3H-(GGGGS)₀-AtFLS1-catalyzed reaction; 4, AtF3H-(GGGGS)₁-AtFLS1-catalyzed reaction; 5, AtF3H-(GGGGS)₂-AtFLS1-catalyzed reaction; 6, AtF3H-(GGGGS)₃-AtFLS1-catalyzed reaction; 7, AtF3H-(GGGGS)₄-AtFLS1-catalyzed reaction. **(C, D)** Polyamide TLC **(C)** and gray density **(D)** analyses of the flavonoid compounds in the AtF3H-(EAAAK)_n-AtFLS1-catalyzed reaction mixture. 8, AtF3H-(EAAAK)₀-AtFLS1-catalyzed reaction; 9, AtF3H-(EAAAK)₁-AtFLS1-catalyzed reaction; 10, AtF3H-(EAAAK)₂-AtFLS1-catalyzed reaction; 11, AtF3H-(EAAAK)₃-AtFLS1-catalyzed reaction; 12, AtF3H-(EAAAK)₄-AtFLS1-catalyzed reaction.

Figure S2. Optimization of various reaction parameters to increase the KMF yield. **(A, B)** Polyamide TLC **(A)** and gray density **(B)** analyses of the flavonoid compounds in each sample for determining the optimum reaction temperature. Digits 1–5 indicate 25 °C, 30 °C, 35 °C, 40 °C, and 45 °C, respectively. **(C, D)** Polyamide TLC **(C)** and gray density **(D)** analyses of the flavonoids in each sample for optimizing the reaction time. Digits 1–7 indicate 0 min, 10 min, 20 min, 30 min, 40 min, 50 min, and 60 min, respectively. **(E, F)** Polyamide TLC **(E)** and gray density **(F)** analyses of each sample for exploring the optimum substrate concentration in the synthetic system. Digits 1–6 indicate 0.05 mM, 0.1 mM, 0.2 mM, 0.3 mM, 0.4 mM, and 0.5 mM, respectively. **(G, H)** Polyamide TLC **(G)** and gray density **(H)** analyses of the flavonoids in each sample for optimizing the total enzyme amount in the synthetic system. Digits 1–5 indicate 5 µg, 10 µg, 15 µg, 20 µg, and 25 µg, respectively. *P < 0.05; **P < 0.01.

Figure S3. Determination of the optimum substrate concentration for AtF3H and AtFLS1. **(A, C)** Polyamide TLC **(A)** and gray density **(C)** analyses of the flavonoids in each sample for determining the optimum substrate concentration in AtF3H-catalyzed reaction. Digits 1–5 indicate 0.1 mM, 0.2 mM, 0.3 mM, 0.4 mM, and 0.5 mM, respectively. **(B, D)** Polyamide TLC **(B)** and gray density **(D)** analyses of the compounds in each sample for exploring the optimum substrate concentration in AtFLS1-catalyzed reaction. Digits 1–5 indicate 0.1 mM, 0.2 mM, 0.3 mM, 0.4 mM, and 0.5 mM, respectively.

Table S1. Oligonucleotide Primers Used in the Current Study.

This material is available as part of the online article from <https://doi.org/10.1590/fst.123922>